Journal of Sound and Vibration (1999) **225**(4), 741–766
Article No. jsvi.1999.2263, available online at http://www.idealibrary.com on IDEAL®

NON-CHAOTIC RESPONSE OF NON-LINEAR OSCILLATORS UNDER COMBINED DETERMINISTIC AND WEAK STOCHASTIC EXCITATIONS

D. ROY

Department of Civil Engineering, Indian Institute of Technology, Kharagpur 721 302, *India*

(*Received* 28 *September* 1998, *and in final form* 18 *March* 1999)

Non-linear oscillators under harmonic and/or weak stochastic excitations are considered in this paper. Under harmonic excitations alone, an analytical technique based on a set of exponential transformations followed by harmonic balancing is proposed to solve for a variety of one-periodic orbits. The stability boundaries for such orbits in the associated parameter space are constructed using the Floquet theory. Under a combination of harmonic and weak stochastic excitations, a stochastic perturbation approach around the deterministic orbit is adopted to obtain response statistics in terms of the evolving moment functions. In the present study, the stochastic perturbation is assumed to be an additive white noise process and equations for the evolving moments are derived using Ito differential rule. A fifth order cumulant neglect closure is used to close the infinite hierarchy of moment equations. Limited numerical results are presented to illustrate the implementation of the proposed scheme. The method is found to be quite versatile and admits ready extensions to Md.o.f. systems under combined harmonic and white or non-white, multiplicative or additive random excitations.
© 1999 Academic Press

1. INTRODUCTION

Even under purely deterministic and periodic excitations, the response of a non-linear oscillator sometimes depends quite sensitively on the choice of parameters and initial conditions. Thus, multiple-periodic, limit-periodic, quasi-periodic, almost-periodic and even choatic motions are possible for different ranges of the associated parameters [1]. A simpler situation, more amenable to analytical solutions, arises when the oscillator responds at the same frequency of the external harmonic forcing function and such a response is generally referred to as one-periodic response. Several analytical tools such as Krylov–Bogoliubov (KB) averaging [2], averaging with Lie series and transforms [3], method of multiple scales [4], harmonic balancing [5], incremental harmonic balancing [6] etc. are available to obtain analytical approximations for one-periodic orbit in terms of known analytic functions. Most of these methods, however, become either too elaborate or inaccurate when the targeted one-periodic orbits in the phase space are asymmetric or markedly non-elliptic. Byatt–Smith [7] has considered an

0022-460X/99/340741 + 26 $30.00/0 © 1999 Academic Press

asymptotic series followed by a multiple time scaling to obtain different periodic orbits of the harmonically forced Duffing–Holmes (DH) oscillator. Such an approach is unfortunately rather too elaborate and requires a numerical effort comparable to that of numerical integrations.

On the other hand, when the oscillator is driven by a combined deterministic and broad-banded stochastic excitation (say, a white noise), the response, in general, is not expected to be stationary. Moreover, for a significantly low intensity of the random noise with uniformly continuous sample paths, the response should be, in a sense, "close" to the one under purely deterministic excitations [8]. An early review on persistence of the topological features of associated deterministic trajectories under random perturbations may be found in the work of Ludwig [9]. In particular, it has been shown that in the limit of the strength of the random noise, modelled as a white noise process, going to zero, the corresponding diffusion equation admits an asymptotic solution, which in turn can be found using the "ray method". The method is essentially a perturbation scheme around that particular ray which represents the deterministic trajectory itself. This leads to a nearly Gaussian estimate for the density function in the vicinity of the deterministic trajectory. The density for larger deviations is obtained based on the minimization of the Lagrangian within a variational framework. Moreover, the question of persistence of trajectories within a given domain with an absorbing boundary may be addressed by constructing an eigenvalue problem for the time-invariant and elliptic diffusion operator. The reciprocal to the first eigenvalue constitutes a measure of the persistence time within the domain. In a recent seminal work, Smelyanksi *et al.* [18] consider the topological pattern of large fluctuations away from a stable limit cycle, surrounding an unstable focus, using an optimal path concept. Given a dynamical system with a stable limit cycle, the approach would be to follow the geometry of the Lagrangian manifold of an auxilliary Hamiltonian system. It is shown that the pattern of the Lagrangian surface near the unstable focus may be many-fold and helicoidal. Projection of these folds on the hyperplane of the auxilliary variables is a caustic, from which extreme paths are reflected. Two caustics meet at a point called cusp. A caustic is not physically observable as it is never reached by an optimal trajectory. Singularities in the form of switching lines between caustics may lead to several attracting zones for the optimal trajectories. It is shown that the zero-energy action near the unstable focus is not exactly quadratic in terms of the distance from the focus and thus the stationary density function near the focus is more complicated than an inverted Gaussian function. Thus, it is concluded that a dynamical system may show up certain "hidden degrees of freedom" when brought close to an unstable fixed point (not necessarily a saddle). Some further work on zero-dispersion non-linear resonance and bifurcation of limit cycles under weak stochastic noise may be found in references [11, 12].

Even though there exists an extensive pool of analytical tools on non-linear oscillators on stationary stochastic excitations [9], no such accurate and widely applicable numerical method is available to handle the non-stationarity that arises due to combined harmonic and stationary stochastic excitations. Thus, such concepts as evolutionary spectral analysis [13] or equivalent linearization with time-dependent frequency response function [14] are not accurate enough to cover

a wide variety of response statistics that may be so characteristic of several non-linear oscillators of engineering interest.

In the present study, an analytical tool based on KB averaging is developed to obtain different types of one-periodic orbits in a class of non-linear oscillators. This is followed by a stability analysis for such orbits via Floquet's theory and construction of corresponding stability diagrams in the parameter space. The problem of a non-linear oscillator under combined harmonic (deterministic) and weak white noise excitation is considered next. Under a weak intensity of the white noise process, a perturbation scheme followed by cumulant neglect closure is proposed to analytically predict a wide class of non-stationary response statistics in terms of their evolving moment functions. A few numerical results are presented to illustrate the effect of a weak stochastic perturbation on a class of non-linear oscillators with a deterministic sinusoidal forcing term. The major advantages and some limitations of the present method, including the important issue of its application to higher-dimensional (Md.o.f.) dynamical systems, are also discussed.

2. THE NONLINEAR OSCILLATORS

Three different non-linear oscillators will be considered at different stages of the present paper. These are the hardening Duffing's (HD), Ueda's and Duffing–Holmes' (DH) oscillators, all of which have cubic non-linearity with or without a linear stiffness term. The HD oscillator, for example, is given by the following second order ordinary differential equation (ODE)

$$\ddot{z} + c\dot{z} + k_1 z + k_2 z^3 = P\cos(\lambda t). \tag{1}$$

Here dots denote differentiation with respect to t and all the five parameters, namely c, k_1, k_2, P and λ, are non-negative real numbers. It is convenient to reduce these five parameters to three via the following set of transformations:

$$x = z/z_c, \qquad z_c = (k_1/k_2)^{1/2}, \qquad \tau = \lambda t/2\pi. \tag{2}$$

This results in

$$x'' + 2\pi\varepsilon_1 x' + 4\pi^2\varepsilon_2(x + x^3) = 4\pi^3\varepsilon_3\cos(2\pi t). \tag{3}$$

Here primes denote differentiation with respect to the non-dimensional time parameter, τ. However, for further discussions, primes would be replaced by dots and τ by t. Ueda's oscillator does not have the linear term in x and is thus represented by

$$\ddot{x} + 2\pi\varepsilon_1\dot{x} + 4\pi^2\varepsilon_2 x^3 = 4\pi^2\varepsilon_3\cos(2\pi t). \tag{4}$$

The DH oscillator, on the other hand, has a negative linear stiffness in x and is given by

$$\ddot{x} + 2\pi\varepsilon_1\dot{x} + 4\pi^2\varepsilon_2(x^3 - x) = 4\pi^2\varepsilon_3\cos(2\pi t). \tag{5}$$

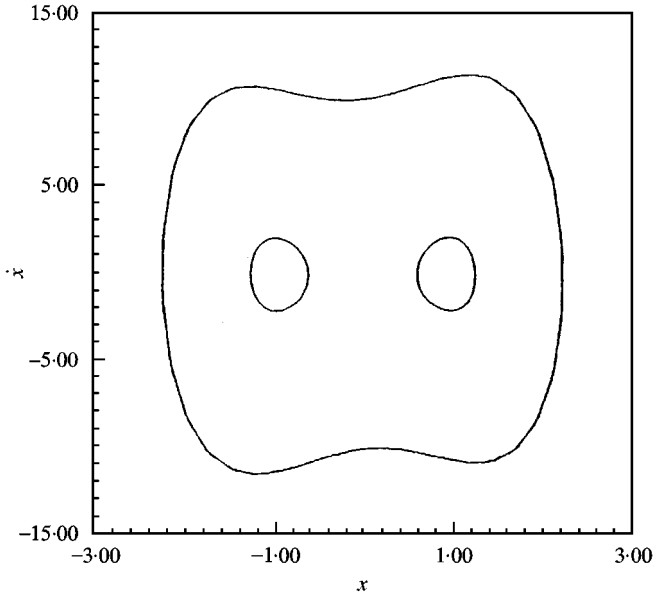

Figure 1. Numerically computed small and large one-periodic orbits for DH oscillator: small orbit: $\varepsilon_1 = 0{\cdot}25$, $\varepsilon_2 = 0{\cdot}5$, $\varepsilon_3 = 0{\cdot}1$; large orbit: $\varepsilon_1 = 0{\cdot}25$, $\varepsilon_2 = 0{\cdot}5$, $\varepsilon_3 = 0{\cdot}60$.

3. ONE-PERIODIC ORBITS

Under harmonic forcing, dissipative non-linear oscillators often respond at the forcing frequency. Such a response is referred to as one-periodic. Several analytical techniques, such as harmonic balancing or KB averaging, are available to efficiently compute one-periodic orbits. Even though an analytical prediction is, at best, only approximate, the advantage of such a procedure lies in that it allows a better insight into the non-linear dynamical characteristics. For all the three oscillators, as mentioned in the last section, one-periodic orbits exist over considerable ranges of parameter values. For example, for sufficiently small values of the forcing amplitude parameter, ε_3, the two stable sinks at $\{\pm 1, 0\}$ for DH oscillator Hopf-bifurcate into a pair of stable one-periodic orbits, encircling each of the singularities at $\{\pm 1, 0\}$. These one-periodic orbits will henceforth be termed "small one-periodic orbits". For still larger values of ε_3, a dumb-bell shaped one-periodic orbit surrounding all the three singularities at $\{\pm 1, 0\}$ and at $\{0, 0\}$ is observed. These dumb-bell shaped orbits will be referred to as "large one-periodic orbits". In Figure 1, numerically computed small and large one-periodic orbits are shown. A similar scenario holds for HD and Ueda's oscillators as well, with the exception that small orbits, in these cases, encircle the singularity at $\{0, 0\}$. As an illustration, Figure 2 shows a few of such typical orbits for Ueda's oscillator. All the orbits, as reported in these two figures, have been obtained using a sixth order Runge–Kutta scheme with a time-step $\Delta t = 0{\cdot}01$. Presently, the possibility of an unified analytical computation for all such orbits is explored.

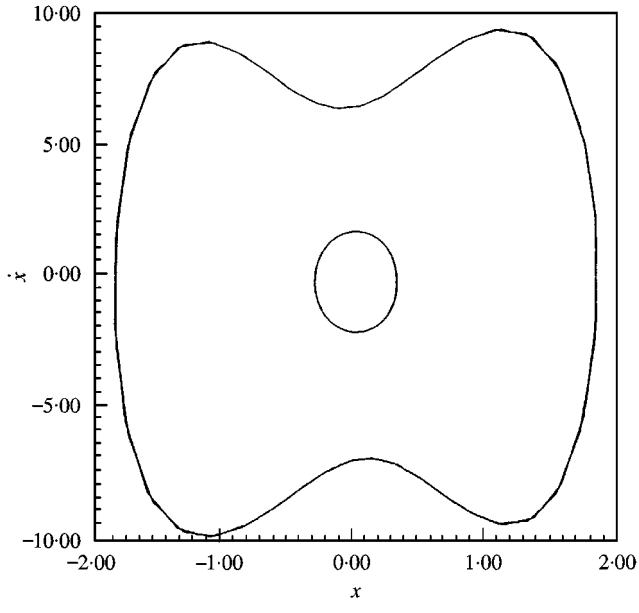

Figure 2. Numerically computed small and large one-periodic orbits for Ueda's oscillator: small orbit: $\varepsilon_1 = 0{\cdot}25$, $\varepsilon_2 = 0{\cdot}5$, $\varepsilon_3 = 0{\cdot}1$; large orbit: $\varepsilon_1 = 0{\cdot}25$, $\varepsilon_2 = 1{\cdot}0$, $\varepsilon_3 = 1{\cdot}5$.

3.1. DH OSCILLATOR

A major difficulty faced in developing an analytical solution for small and large one-periodic orbits is the scarcity of simple analytical expressions, which can closely simulate the shape of such orbits. For the DH oscillator, the solution of a small orbit encircling the sink at $\{1, 0\}$ is taken to be of the form

$$x = \exp(-y), \qquad \dot{x} = -yx \tag{6a}$$

followed by

$$y = C + r\cos(2\pi t - \psi). \tag{6b}$$

Substitution of this equation in the original ODE followed by harmonic balancing results in the following transcendental equation for r:

$$\bar{P}^2\varepsilon_1^2 r^2 + \bar{Q}^2\{r - 2\varepsilon_2 \exp(-2C)I_1(2r)\}^2 = \{\varepsilon_3 \exp(C)\bar{P}\bar{Q}\}^2, \tag{7a}$$

where

$$\exp(-2C) = \frac{(2\varepsilon_2 - r^2)\bar{P} - 2rI_1(r)}{\varepsilon_2\{2I_0(2r)\bar{P} - 4I_1(r)I_1(2r)\}},$$

$$\tan\psi = \frac{\varepsilon_1 r\bar{P}}{\bar{Q}\{r - 2\varepsilon_2 \exp(-2C)I_1(2r)\}},$$

$$\bar{P} = I_0(r) + I_2(r),$$

$$\bar{Q} = I_0(r) - I_2(r). \tag{7b}$$

In the above expressions, I_j denotes the modified Bessel's function of order $j = 0, 1, 2, 3 \ldots$. Similar expressions hold good for the small orbit encircling the other sink at $\{-1, 0\}$ with the exception that x has to be taken in the form

$$x = -\exp(-y). \tag{8}$$

The amplitudes of the large one-periodic orbits are much higher than those of small one-periodic orbits. For most of the parameter ranges, especially for relatively higher values of ε_3, this large orbit is asymmetric. However, for certain parameter values, especially for values of ε_3 immediately above those at which the strange attractor disappears, large one-periodic orbits have a two-sided symmetry in the phase plane. To obtain such solutions, the transformation

$$x = y\exp(y^2) \quad \text{with } y = r\cos 2\pi(t - \psi) \tag{9, 10}$$

is used. Substitution of the above expressions in DH equation (5) followed by harmonic balancing finally leads to the transcendental equation

$$\Gamma_1^2(r) + \Gamma_2^2(r) - 16\pi^4\varepsilon_3^2 = 0. \tag{11}$$

The phase angle ψ is given by

$$\tan(2\pi\psi) = \frac{\Gamma_1(r)}{\Gamma_2(r)}, \tag{12}$$

where

$$\begin{aligned}
\Gamma_1(r) &= 2\pi\varepsilon_1 F_1(r),\\
\Gamma_2(r) &= F_2(r) + 4\pi^2\varepsilon_2\{F_3(r) - F_0(r),\\
F_0(r) &= \{I_0(r^2/2) + I_1(r^2/2)\}r\exp(r^2/2),\\
F_1(r) &= \{-2\pi r\exp(r^2/2) - \pi r^3\exp(r^2/2)\}I_0(r^2/2) + 2\pi r\exp(r^2/2)I_1(r^2/2)\\
&\quad + \pi r^3\exp(r^2/2)I_2(r^2/2) + \ldots,\\
F_2(r) &= -4\pi^2 r\exp(r^2/2)I_0(r^2/2) + 2\pi^2 r^5\exp(r^2/2)I_0(r^2/2)\\
&\quad - 4\pi^2 r\exp(r^2/2)I_1(r^2/2) - 8\pi^2 r^3\exp(r^2/2)I_1(r^2/2)\\
&\quad + \pi^2 r^5\exp(r^2/2)I_1(r^2/2) - 8\pi^2 r^3\exp(r^2/2)I_2(r^2/2)\\
&\quad - 2\pi^2 r^5\exp(r^2/2)I_2(r^2/2) - \pi^2 r^5\exp(r^2/2)I_3(r^2/2) + \ldots,\\
F_3(r) &= 0{\cdot}75r^3\exp(3r^2/2)I_0(3r^2/2) + r^3\exp(3r^2/2)I_1(3r^2/2)\\
&\quad + 0{\cdot}25r^3\exp(3r^2/2)I_2(3r^2/2) + \ldots.
\end{aligned} \tag{13}$$

Here, $I_j(\cdot), j = 0, 1, 2, 3 \ldots$ are the modified Bessel's functions of order j. In deriving the above expressions, the following well-known identity has been made use of:

$$\exp\{r\cos 2\pi(t-\psi)\} = I_0(r) + 2\sum_{j=0}^{\infty} I_j(r)\cos 2\pi j(t-\psi). \tag{14}$$

It may be mentioned that the large one-periodic orbits considered here have a two-sided symmetry about the x- and $\dot{x}$-axis, which intersect at the origin $\{0, 0\}$. Thus, no constant term has been included in equation (10). The present technique is therefore incapable of predicting large asymmetric orbits, especially if the asymmetry is too pronounced.

3.2. UEDA'S AND HD OSCILLATORS

The usual approach for analytical computation of small one-periodic orbits in these cases is to assume

$$x = r\cos 2\pi(t-\psi), \qquad \dot{x} = -2\pi r\sin 2\pi(t-\psi) \tag{15}$$

followed by harmonic balancing or averaging. Such a scheme however fails to predict the large orbits. Here it is of interest to see whether the transformations as in equations (9) and (10) may be used to predict both the small and large one-periodic orbits for these two oscillators. Thus, for example, one has to again solve equations (11) and (12) for r and ψ, which together completely specify the orbit. The expressions for $\Gamma_i(r)$ and $F_i(r)$, as in equation (13), are also the same with the following modifications:

$$\textit{Ueda's}\text{: } F_0(r) = 0, \tag{16a}$$

$$\textit{HD}\text{: } \Gamma_2(r) = F_2(r) + 4\pi^2\varepsilon_2\{F_3(r) + F_0(r). \tag{16b}$$

3.3. STABILITY ANALYSIS

Now that approximate analytical expressions for small and large one-periodic orbits are available, it is necessary to verify whether they are stable solutions for the original dynamical system. This is achieved in the usual way using the linear first variational equation around the approximate periodic orbit followed by a consideration of its eigenvalues. As a further illustration, for the DH oscillator, the linearized and time-variant first variational equation around the periodic orbit is given by

$$\dot{V} = A(t)V, \tag{17}$$

where $V(t) = \{v(t)\cdot \dot{v}(t)\}^{\mathrm{T}}$ is the vector of small variations around the approximate periodic solution and

$$A(t) = \begin{bmatrix} 0 & 1 \\ -4\pi^2\varepsilon_2(3x_p^2 - 1) & -2\pi\varepsilon_1 \end{bmatrix}. \tag{18a}$$

Here $\{x_p(t), \dot{x}_p(t)\}$ denote co-ordinates along the computed periodic orbit projected on the x–$\dot{x}$ plane. Since $A(t)$ is explicitly time-dependant, it is not easy to compute the associated fundamental solution matrix [15]. Equation (17) is therefore converted into a map by numerically solving the equation over one complete cycle of the anticipated one-periodic oscillation. The discrete map so created has a time-step of one full period. The eigenvalues of the associated coefficient matrix for this map are called Floquet multipliers and the analytical solution is obviously stable if the largest multiplier is less than one [15]. The set of parameters for which the highest Floquet multipliers remain less than one forms a boundary in the parameter space. For any choice of parameters within this stability boundary, the response is bound to be one periodic.

Here it is worth mentioning that in certain oscillators with saddle-type connections, such as the DH oscillator, repeated transversal intersections of the stable and unstable manifolds of the saddle often lead to a complicated response, such as chaos. A necessary, but not sufficient, condition for such intersection to take place is that the associated Melnokov function [1] has a zero for some choice of parameters. If zeros of the function can be obtained for different choices of relevant parameters, then a boundary in the parameter space, called the Melnikov boundary, may be constructed. For any choice of parameters within this boundary, the response for the original dynamical system is going to be non-chaotic. In case of DH oscillator, the Melnikov boundary in the $(\varepsilon_3 - \varepsilon_2 - \varepsilon_1)$ space is given by the following equation:

$$\varepsilon_3 = (\varepsilon_1 \sqrt{\varepsilon_2}/24\pi^2) \sinh\{\pi/(2\sqrt{\varepsilon_2})\}. \tag{18b}$$

3.4. NUMERICAL RESULTS

First, the analytically computed one-periodic orbits for the DH oscillator are compared with the numerically simulated orbits in Figure 3. It may be noted that even though the exponential transformations as in equation (6a) are quite useful in closely approximating the egg-shaped actual orbits, the comparison between the simulated and actually orbits is not good for higher values of ε_2. The stability boundary of such orbits, as computed via Floquet's theory, is shown in Figure 5. In Figure 4, a large one-periodic orbit, computed via the transformation in equation (9), is shown and compared against numerical simulation. The comparison is found to be favourable and has been found to be consistent so as long as the actual orbits do not depart too much from the two-sided symmetry. The stability boundaries for these large one-periodic orbits on the ε_3–ε_2 plane, along with the Melnikov boundary (equation 18(b)), is also shown in Figure 5. It is seen that Floquet stability boundaries for periodic orbits delimit the non-chaotic regions in parameter space better than the associated Melnikov boundary. In contrast to the DH oscillator, one-periodic small and large orbits for both Ueda's and HD oscillators share similar characteristics and thus limited results on only Ueda's oscillators are presented in this section. Analytically computed small and large one-periodic orbits for Ueda's oscillator are reported in Figures 6 and 7 along with

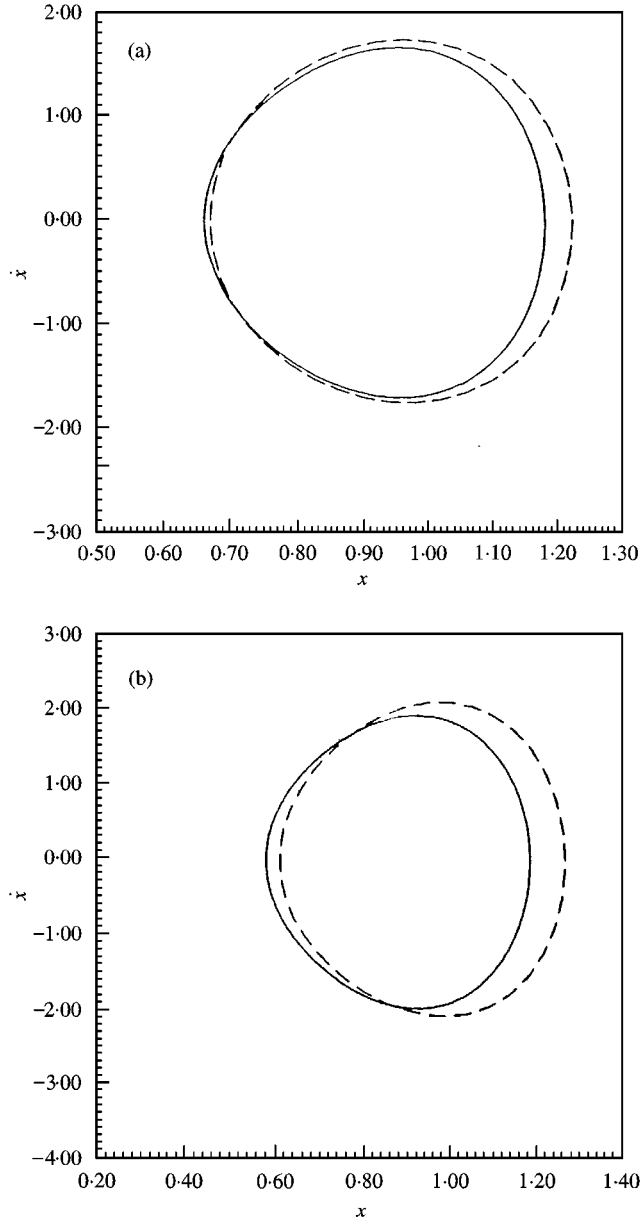

Figure 3. Analytically and numerically computed small one-periodic orbits for DH oscillator: (a) —— Analytical; – – – solution; $\varepsilon_1 = 0{\cdot}25$, $\varepsilon_2 = 0{\cdot}5$, $\varepsilon_3 = 0{\cdot}1$; (b) – – – Simulation; —— analytical. $\varepsilon_1 = 0{\cdot}25$, $\varepsilon_2 = 1{\cdot}0$, $\varepsilon_3 = 0{\cdot}25$.

corresponding results via numerical simulation. The comparisons are again quite favourable as long as the orbits remain symmetric about the x and $\dot{x}$ axes. One typically asymmetric case is shown in Figure 7(c). It may be mentioned that for this case, the highest Floquet multiplier is 0·998, i.e., quite close to 1. Finally, Floquet stability boundaries of all these small and large one-periodic orbits are shown in Figure 8 in the ε_3–ε_2 plane for fixed ε_1.

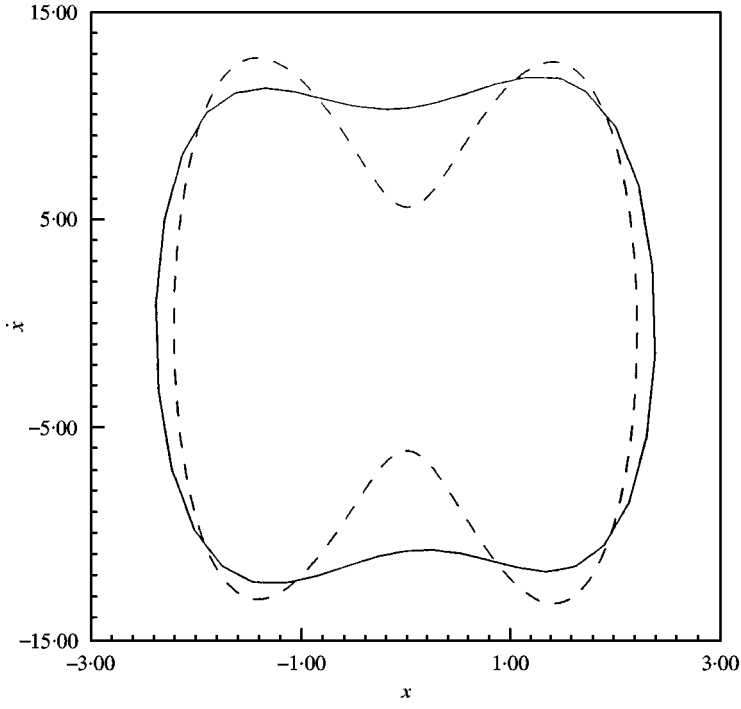

Figure 4. Analytically and numerically computed large one-periodic orbits for DH oscillator: $\varepsilon_1 = 0{\cdot}25$, $\varepsilon_2 = 0{\cdot}5$, $\varepsilon_3 = 0{\cdot}60$. —— Simulation; – – – analytical.

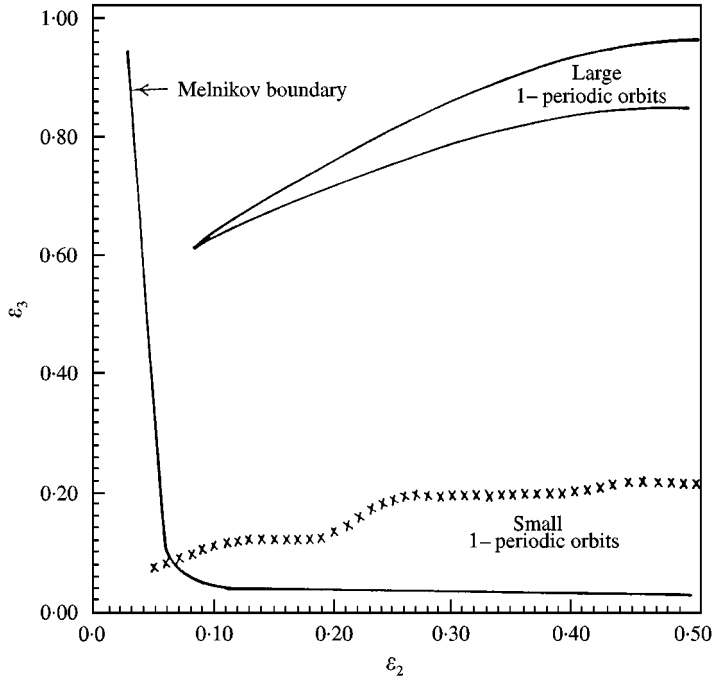

Figure 5. Stable regions of small and large one-periodic orbits for DH oscillator: $\varepsilon_1 = 0{\cdot}25$.

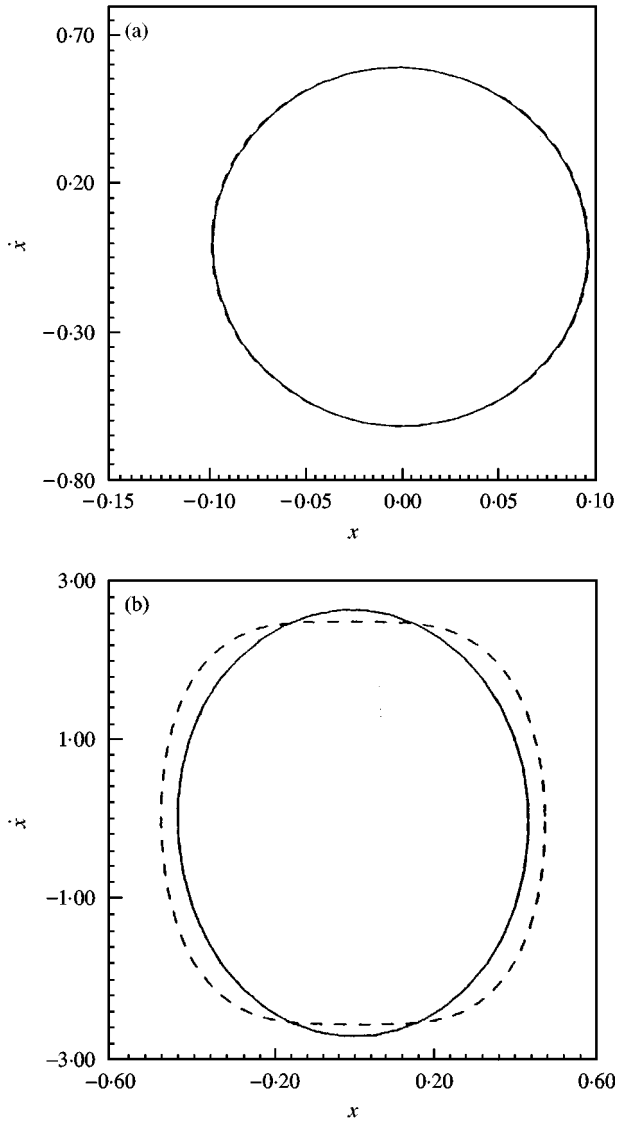

Figure 6. Analytically and numerically computed small one-periodic orbits for Ueda's oscillator: (a) $\varepsilon_1 = 0{\cdot}25$, $\varepsilon_2 = 0{\cdot}5$, $\varepsilon_3 = 0{\cdot}1$; (b) $\varepsilon_1 = 0{\cdot}25$, $\varepsilon_2 = 0{\cdot}5$, $\varepsilon_3 = 0{\cdot}4$. —— Simulation; – – – analytical.

4. COMBINED HARMONIC AND WEAK WHITE NOISE EXCITATIONS

In this section, the effect of a weak stochastic perturbation on the dynamical systems given by equations (3)–(5) is studied using a perturbation scheme followed by some closure approximation. Even though the methodology is illustrated for Sd.o.f. systems and additive white noise perturbations, it admits a very straightforward extension to Md.o.f. oscillators with additive and/or multiplicative

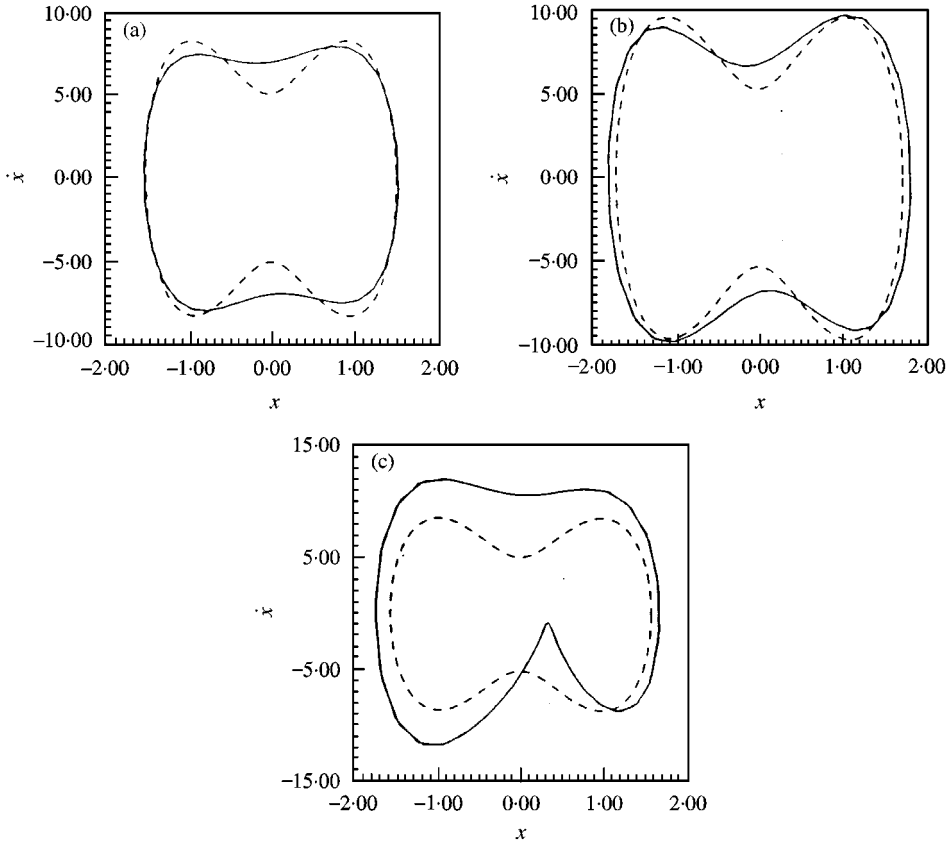

Figure 7. Analytically and numerically computed small one-periodic orbits for Ueda's oscillator: (a) – – – Analytical; —— simulated, $\varepsilon_1 = 0{\cdot}25$, $\varepsilon_2 = 1{\cdot}0$, $\varepsilon_3 = 1{\cdot}5$; (b) —— Simulated; – – – analytical $\varepsilon_1 = 0{\cdot}25$, $\varepsilon_2 = 1{\cdot}0$, $\varepsilon_3 = 2{\cdot}2$; (c) —— Simulated; – – – analytical, $\varepsilon_1 = 0{\cdot}25$, $\varepsilon_2 = 1{\cdot}0$, $\varepsilon_3 = 3{\cdot}8$.

non-white stochastic perturbations. To begin with, the Sd.o.f. oscillators are projected into a state-space vector form as

$$ {}^{\varepsilon}\dot{X} = b({}^{\varepsilon}X, t) + \varepsilon\sigma({}^{\varepsilon}X)\dot{\bar{W}}(t), \tag{19} $$

where ${}^{\varepsilon}X[{}^{s}x\ {}^{s}\dot{x}]$, ε is a real number in [0, 1), $b = [b_1\ b_2]^{\mathrm{T}}$ is the vector valued drift term, σ is the matrix valued diffusion term and $\bar{W} = [0\ W]^{\mathrm{T}}$ is a vector Wiener process. It is known that for $\varepsilon = 0$, the solution of equation (19) exists and is unique [16], whenever b is Lipschitzian, i.e., satisfying a linear growth bound. Since white noise process, which is the formal derivative of a Wiener process, does not have continuous and bounded sample paths, the deterministic theory of existence and uniqueness is not readily extendible for $\varepsilon > 0$. However, for any $t > 0$, if the random variable $\max_{0 \leqslant s \leqslant t} |{}^{\varepsilon}X_{s-}\ X_s|$ is considered, then one can ask whether in the limit as $\varepsilon \to 0$, the probability density of this variable goes to zero or not. Moreover, it is of interest to see whether the second moment of this random variable is bounded for any non-zero $\varepsilon \in (0, 1)$. The following results [8] settle such issues.

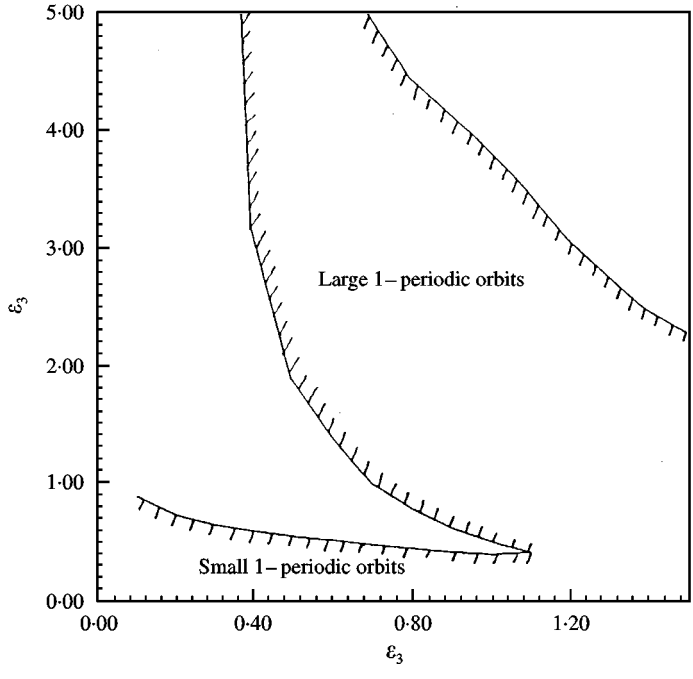

Figure 8. Stable regions of small and large one-periodic orbits for Ueda's oscillator: $\varepsilon_1 = 0{\cdot}25$.

Results 1: Assume that the coefficients of equation (19) satisfy a Lipschitz condition and increase no further than linearly:

$$\sum_{i=1}^{2} [b_i(X) - b_i(Y)]^2 + \sum_{i,j} [\sigma_{ij}(X) - \sigma_{ij}(Y)]^2 \leqslant K^2 |X - Y|^2$$

and

$$\sum_{i=1}^{2} [b_i(X)]^2 + \sum_{i,j} [\sigma_{ij}(X)]^2 \leqslant K^2 |X - Y|^2. \tag{20}$$

Then for all $t > 0$ and $\delta > 0$, one has

$$E|^{\varepsilon}X_t - X_t|^2 \leqslant \varepsilon^2 a(t) \qquad \lim_{\varepsilon \to 0} P\{\max_{0 \leqslant s \leqslant t} |^{\varepsilon}X_s - X_s| > \delta\} = 0, \tag{21a, b}$$

where $a(t)$ is a monotonically increasing function which can be expressed in terms of $|X|$ and the constant K.

In fact, for DH, HD and Ueda's oscillators under combined harmonic and an additive white noise excitation with constant diffusion coefficients, it can be shown via a stochastic Liapunov function approach [17] that all the different moment functions of the perturbed process $^{\varepsilon}X_t$ are bounded in finite time. Now, it is of interest to see whether the following classical perturbation scheme can be used to study the solution of equation (19):

$$^{\varepsilon}X_t = X_t^{(0)} + \varepsilon X_t^{(1)} + \varepsilon^2 X_t^{(2)} + \cdots + \varepsilon^k X_t^{(k)} + {}^{\varepsilon}R^{(k+1)}(t). \tag{22}$$

Here the different constituent processes, $X_t^{(i)}$, are evaluated by substituting equation (22) in equation (19) and equating the various powers of the "smallness parameter" ε. In order to see the applicability of this expansion to the dynamical system (19), the following results by Blagovshchensky [18] are useful.

Results 2: Suppose $b_i(X)$ and $\sigma_{ij}(X)$, $(i, j = 1, 2)$ as in equation (19) have bounded partial derivatives up to order $k + 1$. Then using equation (22) with ε in [0, 1), the random process ${}^{\varepsilon}X_t$ gets approximated to $O(\varepsilon^k)$ if one retains only k terms in the expansion. More precisely, the remainder ${}^{\varepsilon}R^{(k+1)}(t)$ in equation (22) satisfies the inequality

$$\sup_{0 \leqslant t \leqslant T} (E|{}^{\varepsilon}R^{(k+1)}(t)|^2)^{1/2} \leqslant C\varepsilon^{k+1}, \quad C < \infty. \tag{23}$$

It is worth mentioning here that the above results are also valid when the stochastic perturbation is non-white with uniformly continuous sample paths. The interest now is to see how the stochastic perturbation scheme works for the cubic oscillators, as described in section 2, in the simplest case of purely additive white noise excitations with constant (non-random) diffusion coefficients. Towards this, the oscillators are first represented in the following state-space form:

$$\begin{aligned} \dot{x}_1 &= x_2, \\ \dot{x}_2 &= b_2(x_1, x_2, t) + \varepsilon D^{1/2} \dot{W}(t), \end{aligned} \tag{24}$$

where $W(t)$ is a unit Gaussian Wiener process, i.e.,

$$\langle \dot{W}(t) \rangle = 0, \qquad \langle \dot{W}(t_1) \dot{W}(t_2) \rangle = \delta(t_2 - t_1) \tag{25}$$

and the drift term, $b_2(x_1, x_2, t)$, is given by

$$\begin{aligned} b_2 &= -2\pi\varepsilon_1 x_2 - 4\pi^2 \varepsilon_2 x_1^3 + 4\pi^2 \varepsilon_3 \cos(2\pi t) \quad \text{(Ueda's)}, \\ &= -2\pi\varepsilon_1 x_2 - 4\pi^2 \varepsilon_2 (x_1 + x_1^3) + 4\pi^2 \varepsilon_3 \cos(2\pi t) \quad \text{(HD)}, \\ &= -2\pi\varepsilon_1 x_2 - 4\pi^2 \varepsilon_2 (x_1^3 - x_1) + 4\pi^2 \varepsilon_3 \cos(2\pi t) \quad \text{(DH)}. \end{aligned} \tag{26}$$

Use of the perturbation series (19) in equation (24) with b_2 as in HD oscillator, for instance, results in

$$\begin{aligned} \varepsilon^0 &: \dot{x}_1^{(0)} = x_2^{(0)} \\ \dot{x}_2^{(0)} &= -2\pi\varepsilon_1 x_2^{(0)} - 4\pi^2 \varepsilon_2 \{x_1^{(0)} + (x_1^{(0)})^3\} + 4\pi^2 \varepsilon_3 \cos(2\pi t), \end{aligned} \tag{27}$$

$$\begin{aligned} \varepsilon^1 &: \dot{x}_1^{(1)} = x_2^{(1)} \\ \dot{x}_2^{(1)} &= -2\pi\varepsilon_1 x_2^{(1)} - 4\pi^2 \varepsilon_2 x_1^{(1)} - 12\pi^2 \varepsilon_2 (x_1^{(0)})^2 x_1^{(1)} + D^{1/2} \dot{W}(t), \end{aligned} \tag{28}$$

$$\varepsilon^2 : \dot{x}_1^{(2)} = x_2^{(2)}$$

$$\dot{x}_2^{(2)} = -2\pi\varepsilon_1 x_2^{(2)} - 4\pi^2\varepsilon_2 x_1^{(2)} - 12\pi^2\varepsilon_2 (x_1^{(0)})^2 x_1^{(2)} - 12\pi^2\varepsilon_2 x_1^{(0)} (x_1^{(1)})^2. \quad (29)$$

and so on. It may be readily observed that equation (27) is essentially the deterministic non-linear oscillator itself (i.e., without the stochastic perturbation term), for which some analytical solutions for a class of orbits were developed in the last section. Equations (28) and (29), on the other hand, describe the effect of stochastic perturbation. *Thus, using this perturbation scheme, the usefulness of analytical tools is distinctly carried over to the stochastic case as well.* It may also be noted that the conditional vector stochastic process $(x_1^{(1)}, x_2^{(1)} | x_1^{(0)}, x_2^{(0)})$ is jointly Gaussian. For $\varepsilon_3 = 0$, one has $(x_1^{(0)}, x_2^{(0)}) \to (0, 0)$ asymptotically as $t \to \infty$ and thus $(x_1^{(1)}, x_2^{(1)})$ is jointly Gaussian. However, for $\varepsilon_3 \neq 0$, if $x_1^{(0)}(t)$ admits a periodic solution as given by equations (9) and (10), then the information on the phase ψ is lost once the oscillator, given by equation (27), is on the periodic orbit. In this case, ψ can be considered to be a random variable and that $(x_1^{(1)}, x_2^{(1)})$ is non-Gaussian. It is therefore seen that use of terms up to $O(\varepsilon)$ in the perturbation scheme fails to bring in non-Gaussianity in the stationary density function when no harmonic excitation is present. The non-Gaussianity is, however, accounted for in equation (29), which contributes a stochastic correction of $O(\varepsilon^2)$. A careful study of equation (28) also reveals that as $t \to \infty$, one has $\langle x_1^{(1)}(t) \rangle = \langle x_2^{(1)}(t) \rangle = 0$. This is due to a strictly negative viscous damping and a strictly positive coefficient of $x_1^{(1)}$ in equation (28). The first moment of ${}^{\varepsilon}X_t$ is therefore completely determined upto $O(\varepsilon)$ by the deterministic process $X^{(0)}$. On the other hand, equation (29) indeed contributes to $\langle {}^{\varepsilon}X(t) \rangle$ and thus

$$\langle {}^{\varepsilon}X(t) \rangle = \langle X^{(0)}(t) \rangle + \varepsilon^2 \langle X^{(2)}(t) \rangle + O(\varepsilon^3). \quad (30)$$

These observations clearly highlight the importance of $O(\varepsilon^2)$ correction in bringing out the "*non-linear effects*" into the stochastic response of the original oscillator.

4.1. DERIVATION OF MOMENT EQUATIONS

First, the stochastic process, $x_1^{(2)}(t)$, is split up as

$$x_1^2(t) = m_2 + z_2, \qquad m_2 = \langle x_1^2(t) \rangle. \quad (31)$$

This leads to the following ODE and SDE (stochastic differential equation) for m_2 and z_2, respectively,

$$\ddot{m}_2 + 2\pi\varepsilon_1 \dot{m}_2 + 4\pi^2\varepsilon_2 (m_2 + 3(x_1^{(0)})^2 m_2 + 3x_1^{(0)} \langle (x_1^{(1)})^2 \rangle) = 0, \quad (32)$$

$$\ddot{z}_2 + 2\pi\varepsilon_1 \dot{z}_2 + 4\pi^2\varepsilon_2 (z_2 + 3(x_1^{(0)})^2 z_2 + 3x_1^{(0)} ((x_1^{(1)})^2 - \langle (x_1^{(1)})^2 \rangle) = 0. \quad (33)$$

For convenience of deriving ODEs in terms of the moment functions, it is expedient to introduce the following replacements:

$$y_0 = x_1^{(0)}, \qquad y_1 = x_1^{(1)}, \qquad y_2 = x_2^{(1)}, \qquad y_3 = z_2, \qquad y_4 = \dot{z}_2 \tag{34}$$

leading to the following SDEs in y_i, $i = 1, 2, 3, 4$, in state-space form

$$\begin{aligned}
\dot{y}_1 &= y_2, \\
\dot{y}_2 &= -2\pi\varepsilon_1 y_2 - 4\pi^2\varepsilon_2 y_1 - 12\pi^2\varepsilon_2 y_0^2 y_1 + D^{1/2}\dot{W}(t), \\
\dot{y}_3 &= y_4, \\
\dot{y}_4 &= -2\pi\varepsilon_1 y_4 - 4\pi^2\varepsilon_2 y_3 - 12\pi^2\varepsilon_2 y_0^2 y_3 - 12\pi^2\varepsilon_2 y_0(y_1^2 - \langle y_1^2\rangle).
\end{aligned} \tag{35}$$

Due to presence of white noise, the vector process (y_1, y_2, y_3, y_4) is a jointly Markovian vector diffusion process. Moment equations may therefore be derived using the Ito differential rule [11]. For the present study, attention would be restricted to moments up to order 4, i.e., of the type $\langle y_1^i\, y_2^j\, y_3^k\, y_4^l\rangle$, $i, j, k, l = 0, 1, 2, 3, 4$ with $i + j + k + l \leq 4$. Since the first moments $\langle y_i\rangle$, $i = 1, 2, 3, 4$ vanish to zero as $t \to \infty$, it suffices to write down ODEs for the second moment onwards. This exercise leads to 65 first order ODEs, which are partly listed below:

$$\begin{aligned}
\frac{\mathrm{d}}{\mathrm{d}t}\langle y_1^2\rangle &= 2\langle y_1 y_2\rangle, \\
\frac{\mathrm{d}}{\mathrm{d}t}\langle y_2^2\rangle &= -4\pi\varepsilon_1\langle y_2^2\rangle - 8\pi^2\varepsilon_2\langle y_1 y_2\rangle(3x_0^2 + 1) + 2D, \\
\frac{\mathrm{d}}{\mathrm{d}t}\langle y_3^2\rangle &= 2\langle y_3 y_4\rangle, \\
\frac{\mathrm{d}}{\mathrm{d}t}\langle y_4^2\rangle &= -4\pi\varepsilon_1\langle y_4^2\rangle - 8\pi^2\varepsilon_2(\langle y_3 y_4\rangle + 3y_0\langle y_1^2 y_4\rangle + 3y_0^2\langle y_3 y_4\rangle), \\
\frac{\mathrm{d}}{\mathrm{d}t}\langle y_1 y_2\rangle &= \langle y_2^2\rangle - 2\pi\varepsilon_1\langle y_1 y_2\rangle - 4\pi^2\varepsilon_2(\langle y_1^2 + 3y_0^2\langle y_1^2\rangle), \\
\frac{\mathrm{d}}{\mathrm{d}t}\langle y_1 y_3\rangle &= \langle y_2 y_3\rangle + \langle y_1 y_4\rangle, \\
\frac{\mathrm{d}}{\mathrm{d}t}\langle y_1 y_4\rangle &= -2\pi\varepsilon_1\langle y_2 y_3\rangle - 4\pi^2\varepsilon_2\langle y_1 y_3\rangle(1 + 3y_0^2) < y_2 y_4\rangle, \\
\frac{\mathrm{d}}{\mathrm{d}t}\langle y_2 y_3\rangle &= -2\pi\varepsilon_1\langle y_2 y_3\rangle - 4\pi^2\varepsilon_2\langle y_1 y_3\rangle(1 + 3y_0^2) + \langle y_2 y_4\rangle, \\
\frac{\mathrm{d}}{\mathrm{d}t}\langle y_2 y_4\rangle &= -4\pi\varepsilon_1\langle y_2 y_4\rangle - 4\pi^2\varepsilon_1\langle y_1 y_4\rangle + \langle y_2 y_3\rangle) - 12\pi^2\varepsilon_2 y_0(\langle y_1^2 y_2\rangle \\
&\qquad + y_0\langle y_2 y_3\rangle + y_0\langle y_2 y_3\rangle + y_0\langle y_1 y_4\rangle),
\end{aligned}$$

$$\frac{\mathrm{d}}{\mathrm{d}t}\langle y_1^3\rangle = 2\langle y_1^2 y_2\rangle,$$

$$\frac{\mathrm{d}}{\mathrm{d}t}\langle y_1^2 y_2\rangle = 2\langle y_1 y_2^2\rangle - 2\pi\varepsilon_1\langle y_1^2 y_2\rangle - 4\pi^2\varepsilon_2\langle y_1^3\rangle(1 + 3y_0^2),$$

$$\frac{\mathrm{d}}{\mathrm{d}t}\langle y_1^3 y_3\rangle = 2\langle y_1 y_2 y_3\rangle + \langle y_1^2 y_4\rangle,$$

$$\vdots$$

$$\vdots$$

$$\frac{\mathrm{d}}{\mathrm{d}t}\langle y_3^4\rangle = 4\langle y_3^3 y_4\rangle,$$

$$\frac{\mathrm{d}}{\mathrm{d}t}\langle y_3^3 y_4\rangle = 3\langle y_3^2 y_4^2\rangle - 2\pi\varepsilon_1\langle y_3^3 y_4\rangle - 4\pi^2\varepsilon_2\langle y_3^4\rangle(1 + 3y_0^2)$$
$$- 12\pi^2\varepsilon_2 y_0(\langle y_1^2 y_3^3\rangle - \langle y_1^2\rangle\langle y_3^3\rangle),$$

$$\frac{\mathrm{d}}{\mathrm{d}t}\langle y_3^2 y_4^2\rangle = 2\langle y_3 y_4^3\rangle - 4\pi\varepsilon_1\langle y_3^2 y_4^2\rangle - 8\pi^2\varepsilon_2\langle y_3^3 y_4\rangle(1 + 3y_0^2)$$
$$- 24\pi^2\varepsilon_2 y_0(\langle y_1^2 y_2^2 y_4\rangle - \langle y_1^2\rangle\langle y_2^2 y_4\rangle),$$

$$\frac{\mathrm{d}}{\mathrm{d}t}\langle y_3 y_4^3\rangle = \langle y_4^4\rangle - 6\pi\varepsilon_1\langle y_3 y_4^3\rangle - 12\pi^2\varepsilon_2\langle y_3^2 y_4^2\rangle(1 + 3y_0^2)$$
$$- 36\pi^2\varepsilon_2 y_0(\langle y_1^2 y_3 y_4^2\rangle - \langle y_1^2\rangle\langle y_3 y_4^2\rangle),$$

$$\frac{\mathrm{d}}{\mathrm{d}t}\langle y_4^4\rangle = -8\pi\varepsilon_1\langle y_4^4\rangle - 16\pi^2\varepsilon_2\langle y_3 y_4^3\rangle(1 + 3y_0^2)$$
$$- 36\pi^2\varepsilon_2 y_0(\langle y_1^2 y_4^3\rangle - \langle y_1^2\rangle\langle y_4^3\rangle). \tag{36}$$

Since the system of equations (35) is non-linear, the set of moment equations (36) is not closed in that it contains fifth order moments of the type $\langle y_1^i y_2^j y_3^k y_4^l\rangle$ with $i + j + k + l = 5$. It is here that a closure approximation is called for so that these higher order moments can be approximately replaced by a suitable combination of lower order ones.

4.2. A CUMULANT NEGLECT CLOSURE

It is well known that unlike the statistical moments, various cumulants (alternatively known as semi-invariants) of increasingly higher orders form a

non-increasing sequence [9]. Moreover, it is expected that the physical significance of a cumulant decreases as the order increases and the most important properties of a random process are revealed in the lower order cumulants [19]. Here, it is assumed that the cumulants of the order higher than 4 are all zero. This is then a fifth order cumulant neglect approximation and leads to the following algebraic equations for closure:

$$\langle y_1^5\rangle = 10\langle y_1^2\rangle\langle y_1^3\rangle,$$

$$\langle y_1^4 y_2\rangle = 5(\langle y_1^3\rangle\langle y_1 y_2\rangle + \langle y_1^2\rangle\langle y_1^2 y_2\rangle),$$

$$\langle y_1^4 y_3\rangle = 5(\langle y_1^3\rangle\langle y_1 y_3\rangle + \langle y_1^2\rangle\langle y_1^2 y_3\rangle),$$

$$\langle y_1^4 y_4\rangle = 5(\langle y_1^3\rangle\langle y_1 y_4\rangle + \langle y_1^2\rangle\langle y_1^2 y_4\rangle),$$

$$\langle y_1^3 y_2^2\rangle = \tfrac{10}{3}(\langle y_1^3\rangle\langle y_2^2\rangle + \langle y_1^2\rangle\langle y_1 y_2^2\rangle + \langle y_1 y_2\rangle\langle y_1^2 y_2\rangle),$$

$$\langle y_1^3 y_2 y_3\rangle = \tfrac{5}{2}(\langle y_1^3\rangle\langle y_2 y_3\rangle + \langle y_1^2\rangle\langle y_1 y_2 y_3\rangle + \langle y_1^2 y_2\rangle\langle y_1 y_3\rangle + \langle y_1^2 y_3\rangle\langle y_1 y_2\rangle),$$

$$\langle y_1^3 y_2 y_4\rangle = \tfrac{5}{2}(\langle y_1^3\rangle\langle y_2 y_4\rangle + \langle y_1^2\rangle\langle y_1 y_2 y_4\rangle + \langle y_1^2 y_2\rangle\langle y_1 y_4\rangle + \langle y_1^2 y_4\rangle\langle y_1 y_2\rangle),$$

$$\langle y_1^3 y_3^2\rangle = \tfrac{10}{3}(\langle y_1^3\rangle\langle y_3^2\rangle + \langle y_1^2\rangle\langle y_1 y_3^2\rangle + \langle y_1 y_3\rangle\langle y_1^2 y_3\rangle),$$

$$\langle y_1^3 y_3 y_4\rangle = \tfrac{5}{2}(\langle y_1^3\rangle\langle y_3 y_4\rangle + \langle y_1^2\rangle\langle y_1 y_3 y_4\rangle + \langle y_1^2 y_3\rangle\langle y_1 y_4\rangle + \langle y_1^2 y_4\rangle\langle y_1 y_3\rangle),$$

$$\langle y_1^3 y_4^2\rangle = \tfrac{10}{3}(\langle y_1^3\rangle\langle y_4^2\rangle + \langle y_1^2\rangle\langle y_1 y_4^2\rangle + \langle y_1 y_4\rangle\langle y_1^2 y_4\rangle),$$

$$\langle y_2^3 y_1^2\rangle = \tfrac{10}{3}(\langle y_2^3\rangle\langle y_1^2\rangle + \langle y_2^2\rangle\langle y_2 y_1^2\rangle + \langle y_1 y_2\rangle\langle y_2^2 y_1\rangle),$$

$$\begin{aligned}\langle y_1^2 y_2^2 y_3\rangle = 2(&\langle y_1^2\rangle\langle y_2^2 y_3\rangle + \langle y_1^2 y_3\rangle\langle y_2^2\rangle + \langle y_2 y_3\rangle\langle y_1^2 y_2\rangle + \langle y_1 y_2\rangle\langle y_1 y_2 y_3\rangle\\ &+ \langle y_1 y_3\rangle\langle y_2^2 y_1\rangle),\end{aligned}$$

$$\begin{aligned}\langle y_1^2 y_2^2 y_4\rangle = 2(&\langle y_1^2\rangle\langle y_2^2 y_4\rangle + \langle y_1^2 y_4\rangle\langle y_2^2\rangle + \langle y_2 y_4\rangle\langle y_1^2 y_2\rangle + \langle y_1 y_2\rangle\langle y_1 y_2 y_4\rangle\\ &+ \langle y_1 y_4\rangle\langle y_2^2 y_1\rangle),\end{aligned}$$

$$\begin{aligned}\langle y_1^2 y_3^2 y_2\rangle = 2(&\langle y_1^2\rangle\langle y_3^2 y_2\rangle + \langle y_1^2 y_2\rangle\langle y_3^2\rangle + \langle y_2 y_3\rangle\langle y_1^2 y_3\rangle + \langle y_1 y_3\rangle\langle y_1 y_2 y_3\rangle\\ &+ \langle y_1 y_2\rangle\langle y_3^2 y_1\rangle),\end{aligned}$$

$$\begin{aligned}\langle y_1^2 y_2 y_3 y_4\rangle = \tfrac{10}{7}(&\langle y_1^2\rangle\langle y_2 y_3 y_4\rangle + \langle y_1^2 y_2\rangle\langle y_3 y_4\rangle + \langle y_1^2 y_3\rangle\langle y_2 y_4\rangle\\ &+ \langle y_1^2 y_4\rangle\langle y_2 y_3\rangle + \langle y_1 y_2\rangle\langle y_1 y_3 y_4\rangle + \langle y_1 y_3\rangle\langle y_1 y_2 y_4\rangle\\ &+ \langle y_1 y_4\rangle\langle y_1 y_2 y_3\rangle.\end{aligned} \tag{37}$$

Use of the above set of relationship in equation (36) results in a closed set of non-linear moment equations which can be integrated numerically.

4.3. NUMERICAL RESULTS

Equations (36) have been solved together with equations (27) and (32) to obtain the evolving moment flows up to order 4. For numerical integration, a sixth order Runge–Kutta scheme with a step size of 0·01 has been made use of. First, as a check, only the HD oscillator under white noise excitation is considered. In this and all the following examples, the parameter ε has been assigned the value 1 without any loss of generality. The stationary variance of the process ${}^{\varepsilon}x(t)$, henceforth called $x(t)$ for simplicity, is plotted in Figure 9. The plotted variance is seen to be quite close to the exact variance of 0·016. The case of combined white noise and harmonic excitations is considered next. Towards this a small one-periodic (deterministic) orbit is first shown in Figure 10(a), and the effect of stochasticity in the phase plane of mean of the process $x(t)$ and its derivative $\dot{x}(t)$ is reported in the same figure. The $O(\varepsilon^2)$ stochastic correction is pretty clear. Evolutions of variances of the processes $x(t)$ are shown in Figures 10(b) and 10(c) respectively. It may be pointed out that instead of solving equation (27) numerically, transformations (9) and (10) may be directly under to solve for this equation in the one-periodic regime. In Figure 11, similar results as in figure (10) are reported for the case when the deterministic part of the oscillator admits a large one-periodic orbit. In Figures 12–14, the phase plane structure of the mean and its derivative along with evolutions of variances are shown for certain multi-periodic cases. It is readily observed that the effect of $O(\varepsilon^2)$ stochastic correction to the mean may sometimes be quite considerable.

The present scheme is however unable to yield converged estimates of evolving moment functions when the parameters are so chosen that the deterministic part of the oscillator is in the chaotic regime. The fault here probably lies with the closure

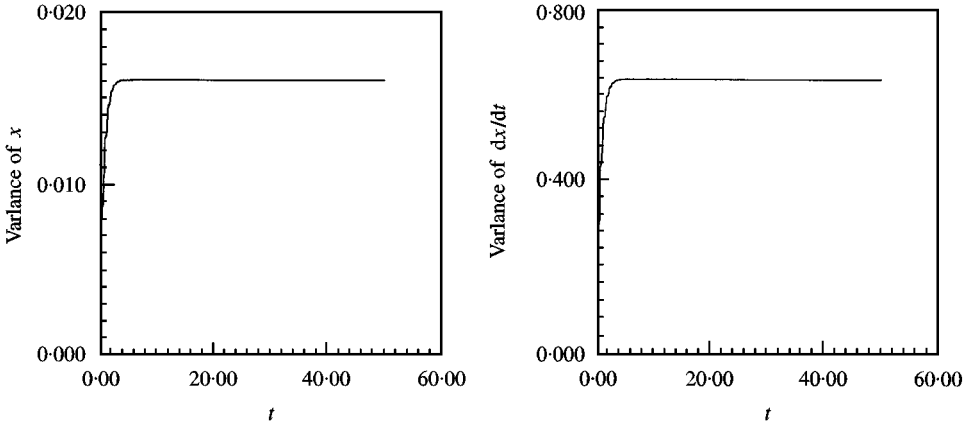

Figure 9. Response variances of DH oscillator only under white noise: $\varepsilon_1 = 0{\cdot}25$, $\varepsilon_2 = 1{\cdot}0$, $D = 0{\cdot}1$.

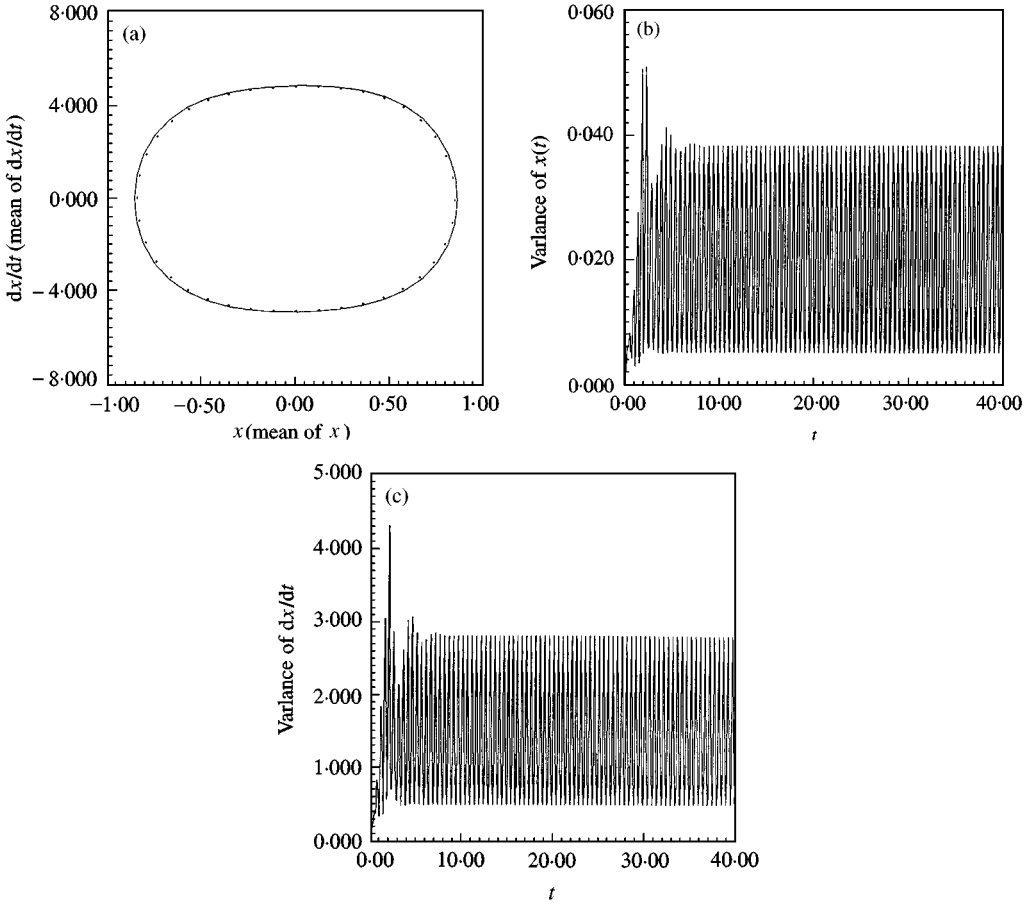

Figure 10. Response of DH oscillator under harmonic and/or stochastic excitations, $\varepsilon_1 = 0{\cdot}25$, $\varepsilon_2 = 1{\cdot}0$, $\varepsilon_3 = 0{\cdot}1$, $D = 0{\cdot}1$. (a) Phase plot —— Only harmonic excitation, $\cdots$ combined harmonic and random excitation; (b) evolving variance of x; (c) evolving variance of $\dot{x}$.

approximation, which fails to catch the locally unstable nature of each of the realizations of evolving trajectories.

Precisely, similar developments as reported in sections 4.1, 4.2 and this section so far, hold true for DH and Ueda's oscillators as well. Results for these two cases are therefore not reported explicitly in the present study.

5. DISCUSSIONS AND CONCLUSIONS

A few analytical approaches for studying a class of deterministic and a wider class of stochastic response of some non-linear Sd.o.f. oscillators are presented in this paper. In case of oscillators driven only by harmonic excitation, certain transformations are proposed to analytically obtain various types of symmetric one-periodic orbits. The stability boundaries for such orbits have also been studied

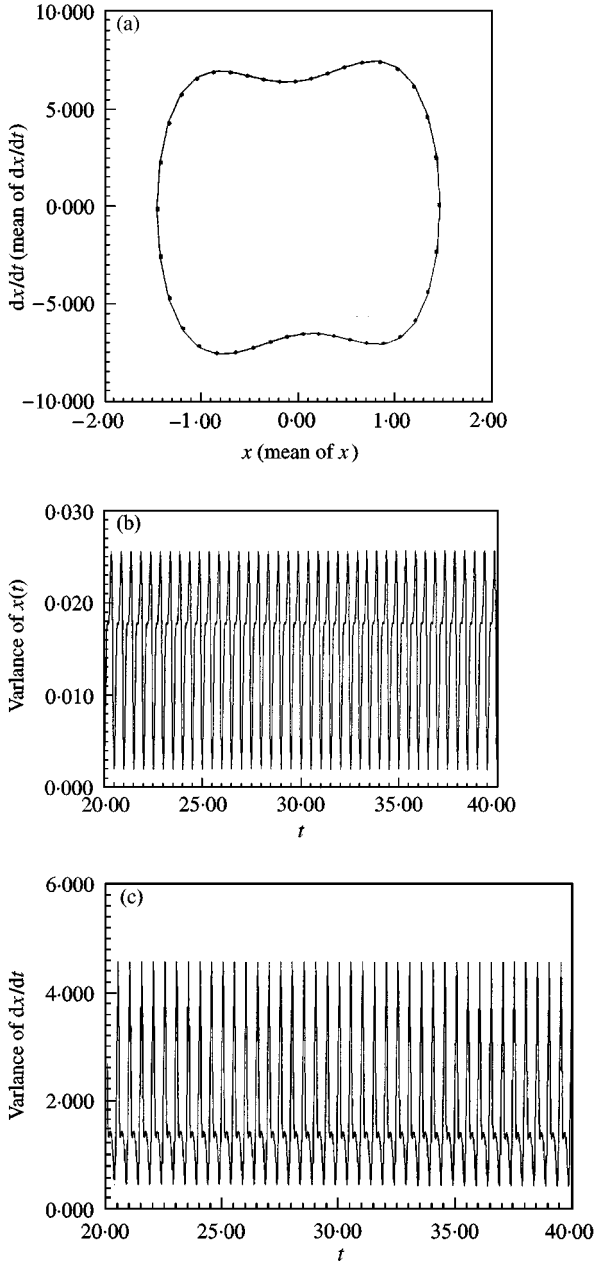

Figure 11. Response of DH oscillator under harmonic and/or stochastic excitations, $\varepsilon_1 = 0{\cdot}25$, $\varepsilon_2 = 1{\cdot}0, \varepsilon_3 = 9{\cdot}0, D = 0{\cdot}1$. (a) Phase plot —— Only harmonic excitation, $\cdots$ combined harmonic and random excitation; (b) evolving variance of x; (c) evolving variance of $\dot{x}$.

using Floquet's theory and these boundaries have been plotted in the associated parameter space. The problem of finding the stochastic response of non-linear oscillators under combined harmonic and weak white noise excitations is next dealt with via a stochastic perturbation approach. First, mathematical justifications for

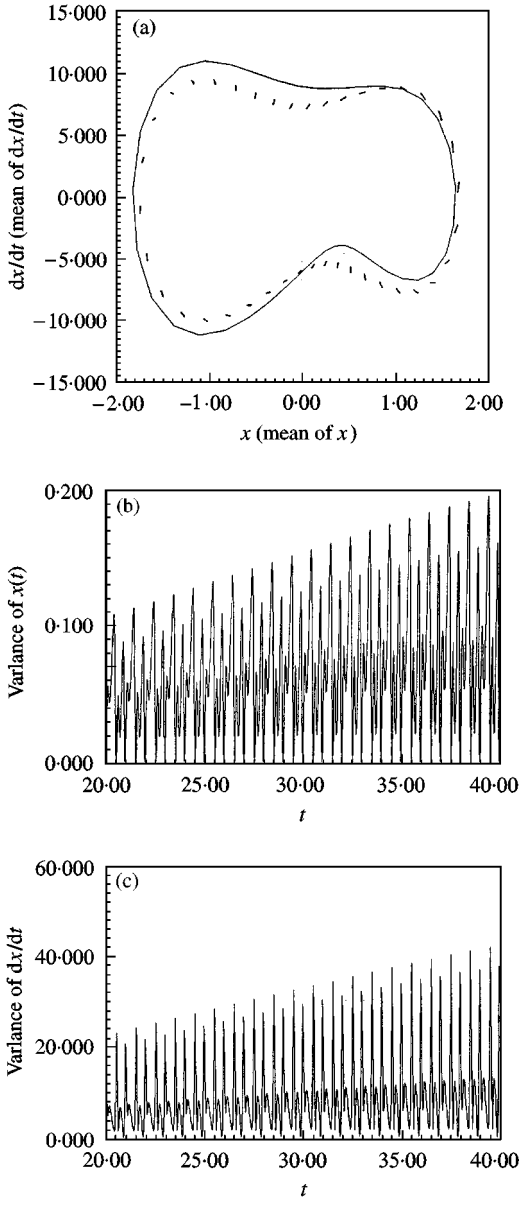

Figure 12. Response of DH oscillator under harmonic and/or stochastic excitations, $\varepsilon_1 = 0{\cdot}25$, $\varepsilon_2 = 1{\cdot}0$, $\varepsilon_3 = 11{\cdot}1$, $D = 0{\cdot}1$. (a) Phase plot —— Only harmonic excitation, $\cdots$ combined harmonic and random excitation; (b) evolving variance of x; (c) evolving variance of $\dot{x}$.

such an approach is provided in terms of boundedness of evolving moment functions as well as vanishing of probability distribution of the random process, denoting the difference between randomly perturbed and unperturbed response processes in the limit of the strength of random forcing function going to zero. Implementation of the proposed scheme is then illustrated for a class of simple Sd.o.f. non-linear oscillators. *The method has the advantage of uncoupling the*

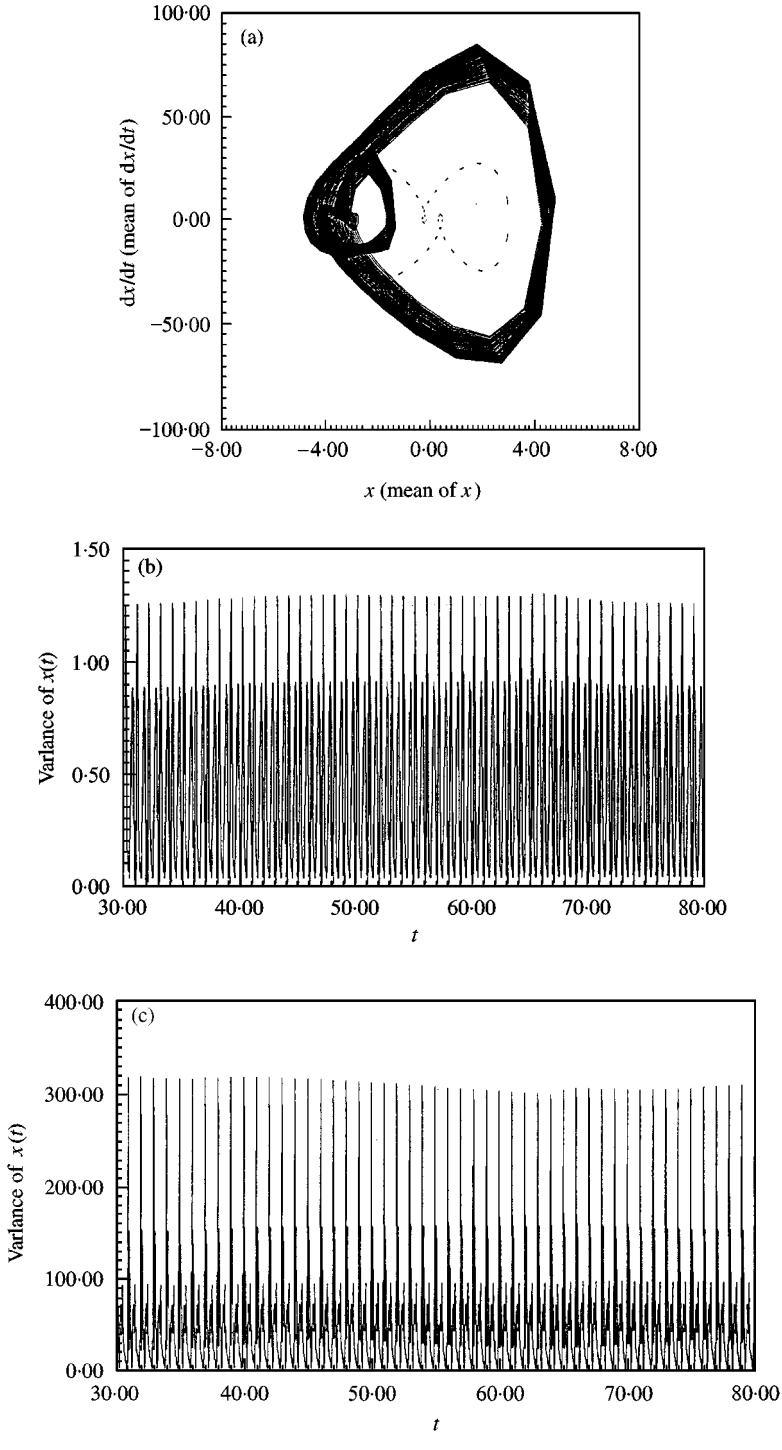

Figure 13. Response of DH oscillator under harmonic and/or stochastic excitations, $\varepsilon_1 = 0{\cdot}25$, $\varepsilon_2 = 1{\cdot}0$, $\varepsilon_3 = 5{\cdot}8$, $D = 0{\cdot}1$. (a) Phase plot —— Combined harmonic and random excitation; $\cdots$ only harmonic excitation; (b) evolving variance of x; (c) evolving variance of $\dot{x}$.

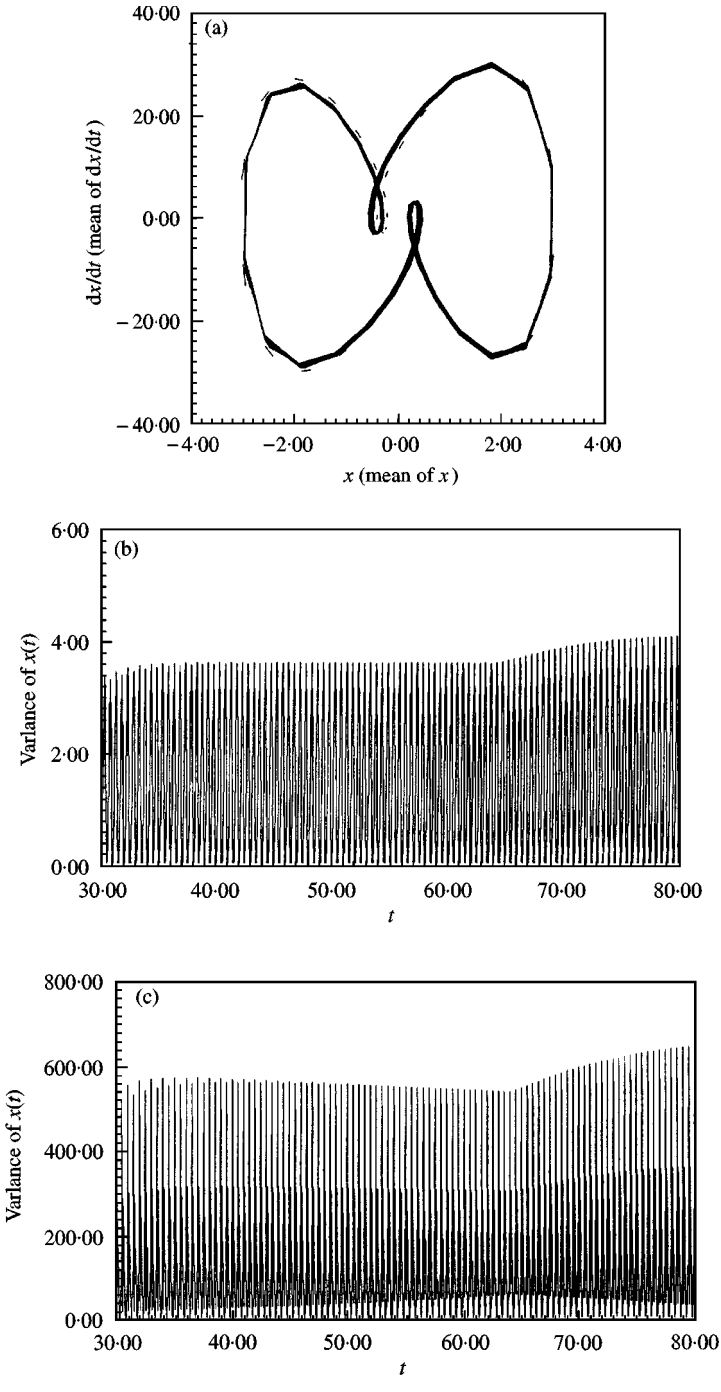

Figure 14. Response of DH oscillator under harmonic and/or stochastic excitations, $\varepsilon_1 = 0{\cdot}25$, $\varepsilon_2 = 1{\cdot}0$, $\varepsilon_3 = 5{\cdot}8$, $D = 0{\cdot}05$. (a) Phase plot —— Only harmonic excitation, $\cdots$ combined harmonic and random excitation; (b) evolving variance of x; (c) evolving variance of $\dot{x}$.

deterministic part of the response process from the stochastic part, which is actually coupled with the deterministic part. The approach enables one to precisely study the stochastic correction to known deterministic solutions due to weak random excitations. If ε denotes, in a sense, strength or intensity of the noise process, then terms up to $O(\varepsilon)$ in the perturbation series predict only the nearest Gaussian estimate. However, non-Gaussian corrections, so characteristic of non-linear oscillators even under Gaussian inputs, are predicted by terms of $O(\varepsilon^2)$ and higher. Since the noise process in the present study has been restricted to white noise only, ODEs for moment equations have been derived using the well-known Ito calculus. The problem being non-linear, these equations constitute an infinite hierarchy and naturally call for a suitable closure approximation. A fifth order cumulant neglect closure has been adopted for the present study. *It has been found that the closure approximation gives convergent and accurate estimates of moments, provided that the associated response is not in the chaotic regime*. Unfortunately, a suitable closure scheme in the chaotic regime still remains an unresolved issue.

An additional advantage in the stochastic perturbation approach is its rather straightforward extension to Md.o.f. nonlinear systems of engineering interest under white or non-white random excitations. Of similar interest would be the case where the stochastic excitation is in the form of Poisson's white noise or a general α-stable process. Another important question not dealt with here is that of stochastic stability of the analytical solutions. These issues require further investigations and will be taken up elsewhere.

ACKNOWLEDGMENTS

The author wishes to acknowledge some useful discussions with Prof. R. N. Iyengar, Director of Central Building Research Institute, Roorkee 247 667, India. Thanks are also due to the referees for some of their very useful comments.

REFERENCES

1. J. Guckenheimer and P. Holmes 1983 *Nonlinear Oscillations, Dynamical Systems and Bifurcations of Vector Fields*. New York: Springer.
2. M. Struble 1962 *Nonlinear Differential Equations*. New York: McGraw Hill.
3. A. A. Kamel 1970 Celestial Mech., **3**, 92–106. Perturbation method in the theory of nonlinear oscillations.
4. H. Nayfeh and D. T. Na Mook 1979 *Nonlinear Oscillations*. New York: Wiley.
5. C. Hayashi 1964 *Nonlinear Oscillations in Physical Systems*. New York: McGraw Hill.
6. S. L. Lau, Y. K. Cheung and S. Y. Wu 1983 *Journal of Applied Mechanics* **50**, 871–876. Incremental harmonic balancing method with multiple time scales for a periodic vibrations of nonlinear systems.
7. J. G. Byatt-Smith 1987 *SIAM Journal of Applied Mathematics* **47**, 60–91. 2π periodic solutions of Duffing's equation with negative stiffness'.
8. M. I. Friedlin and A. D. Wentzell 1984 Random Perturbations of Dynamical Systems. New York: Springer.
9. D. Ludwig 1975 *SIAM Review* **17**, 605–640. Persistence of Dynamical Systems under Random Perturbations.

10. V. N. Smelyanskiy, M. I. Dykman and R. S. Maier 1997 *Physical Review E* **55**, 2369–2391. Topological features of large fluctuations to the interior of a limit cycle.
11. D. G. Luchinsky, P. V. E. McClintock, S. M. Soskin and R. Mannella 1996 *Physical Review Letters*. **76**, 4453–4457. Zero-dispersion nonlinear resonance in dissipative systems.
12. R. Mannella, S. M. Soskin and P. V. E. McClintock 1998 *International Journal of Bifurcation and Chaos* **8**, 701–712. Bifurcation analysis of zero-dispersion nonlinear resonance.
13. M. Shinozuka and P. Brant 1969 *Proceedings ASCE-EMD Speciality Conference on Probabilistic Concepts and Methods in Engineering*, *Purdue University*, *West Lafayette*, *Ind*., *November* 12–14, 42–46. Application of the evolutionary power spectrum in structural dynamics.
14. J. B. Roberts 1984 *Shock and Vibration Digest*. **13**, 15–29. Techniques for nonlinear random vibration problems.
15. P. Hartman 1964 *Ordinary Different Equations*. New York: McGraw Hill.
16. E. L. Coddington and N. Levinson 1995 *Theory of Ordinary Differential Equations*. New York: McGraw Hill.
17. D. Roy 1996 *Report of Institute of Engineering Mech*., *Univ. Of Innsbruck*, *Austria*, *Under grant (FWF) 11498-MAT*. A new pathwise linearisation method for nonlinear oscillators.
18. Yu. N. Blagoveshchensky 1962 *Theory Probability and its Applications* **7**, 135–152. Diffusion processes depending on a small parameter (translated in English).
19. Y. K. Lin and G. Q. Cai 1995 *Probabilistic Structural Dynamics: Advanced Theory and Applications.* New York: McGraw Hill.
20. R. A. Ibrahim, A. Soundararajan and H. Heo 1985 *Journal of Applied Mechanics* **52**, 965–970. Stochastic response of nonlinear dynamic systems based on a non-Gaussian closure.
21. V. S. Pugachev and I. N. Sinitsyn 1987 *Stochastic Differential Systems: Analysis and Filtering.* Chichester: Wiley.
22. T. T. Soong and M. Grigoriu 1993 *Random Vibration of Mechanical and Structural Systems*. Englewood Cliffs, NJ: Prentice-Hall.